Available online at www.sciencedirect.com
ScienceDirect
Acta Materialia 55 (2007) 3253–3260
Acta MATERIALIA
www.elsevier.com/locate/actamat

Measurement of deformations in SnAgCu solder interconnects under in situ thermal loading

Seungbae Park [a,*], Ramji Dhakal [a], Lawrence Lehman [b], Eric Cotts [b]

[a] Mechanical Engineering Department, Binghamton University, Binghamton, NY 13902, USA
[b] Physics Department, Binghamton University, Binghamton, NY 13902, USA

Received 2 August 2006; received in revised form 19 January 2007; accepted 20 January 2007
Available online 23 March 2007

Abstract

Optical microscopy was used to discern the different grain orientations and grain boundaries on the polished cross-sections of near-eutectic lead-free board-level SnAgCu (SAC) solder interconnects. Strain distributions with submicron accuracy of the deformations on the cross-sections of the solder interconnects were measured when the package was subjected to thermal loading from room temperature to 100 °C. The results were correlated with the locations of different grains, grain boundaries and larger primary intermetallics. It revealed anisotropic nature of deformations in different grains of the SAC solder, which is similar to the thermomechanical behavior of pure Sn. The strain distribution in a solder interconnect varied significantly in different grain orientations. The primary intermetallics (Ag_3Sn plates) also behaved very differently from the surrounding Sn matrix under the thermal loading. The demonstrated strain localization along the grain boundaries and bigger primary intermetallics provides a clue for the path of fatigue crack growth that leads to a failure because of anisotropic thermomechanical response of SAC solder during thermal cycling.
© 2007 Acta Materialia Inc. Published by Elsevier Ltd. All rights reserved.

Keywords: Pb-free; SnAgCu; Grain boundary; BGA

1. Introduction

It is well known that tin (Sn) exhibits anisotropy in thermomechanical behaviors [1–5]. Accordingly, the primarily Sn-based, near-eutectic SnAgCu (SAC) interconnects, which typically possess a few grains, have similar anisotropic properties [6–8] in board-level ball grid array (BGA) interconnects. It is reported that SAC solders do not fail in the same way as the Pb–Sn interconnects. A better understanding of the failure mechanisms of such solder interconnects is required for the construction of more realistic Pb-free solder reliability models.

The linear coefficient of thermal expansion (CTE) of body-centered tetragonal β-tin along the [0 0 1] axis (*c*-axis) is reported to be about twice that along the [1 0 0] (*a*-axis) and [0 1 0] axes (*b*-axis). Similarly, the Young's modulus along the *c*-axis is about three times larger than that along the *a*- and *b*-axes [3,4]. Sn grains are very often twinned, with twinning angles near 60° around the [0 1 0] axis. This implies that the orientations of these grains in a multi-grain solder interconnect may be highly correlated [8,9]. In SAC solder interconnects, this large-grained Sn matrix contains Cu_6Sn_5 and Ag_3Sn intermetallic precipitates, whose size depends on solder composition and reflow conditions. The inherent large anisotropies in the thermomechanical properties of Sn and the differences in the mechanical properties of Sn and intermetallic precipitates in a SAC solder joint lead to a failure mechanism quite different from that of a Pb–Sn joint.

On the other hand, because of a higher percentage of softer Pb phase in Pb–Sn solder alloy, it is more compliant to deformations, and its response to thermomechanical loading can be assumed to be homogeneous and isotropic. Several studies have demonstrated that the failure of a SAC solder interconnect is governed not only by its location in

* Corresponding author. Tel.: +1 607 777 3415; fax: +1 607 777 4620.
E-mail address: sbpark@binghamton.edu (S. Park).

1359-6454/$30.00 © 2007 Acta Materialia Inc. Published by Elsevier Ltd. All rights reserved.
doi:10.1016/j.actamat.2007.01.028

terms of the distance from the neutral point (DNP) of an assembly but also by the orientation and number of grains [1–4] in the interconnect. In thermal cycling experiments, the fatigue cracks have been observed propagating along the Sn grain boundaries, solder–pad interfaces and also along the Sn/primary intermetallics interfaces [2,3,10].

To characterize the thermomechanical response and, hence, the failure mechanism of SAC solder interconnects, it is vital to understand the interaction between the grains of different orientations when the interconnect is thermomechanically stressed, and also the role of larger primary intermetallics in the failure of such interconnects.

This study employs an innovative combination of optical tools to examine the microstructure and strain distribution in the Pb-free SAC solder interconnects. Bright-field (BF) and cross-polarizer (XP) imaging techniques of optical microscopy have been used to discern the different grains in the cross-sections. Digital image correlation (DIC) [11–13] has been used to quantify deformation and strain, resulting from a thermal loading, on the solder interconnects. These measured strains are correlated with Sn grains, grain boundaries and larger intermetallic precipitates to study the role of different grain orientations and larger primary intermetallics in the failure mechanism.

2. Experiment

2.1. Sample preparation and set-up

A flip-chip plastic ball grid array (PBGA) package in a 20×20 ball grid array (BGA) (CASTIN alloy: Sn–2.5Ag–0.8Cu–0.5Sb) and a flip-chip ceramic ball grid array (CBGA) package in a 25×25 BGA (Sn–3.8Ag–0.7Cu) of lead-free board-level interconnects in 1.27 mm pitch were sectioned to produce strips with four rows of solder interconnects. The first row in each strip of solder interconnects was manually ground and polished flat without mounting on an epoxy. The final surface, which consisted of fine Sn dendrites decorated with intermetallic precipitates, provided a random variation of grayscale in the BF images of the cross-section, which is an important requirement of DIC. Sample preparation and DIC technique are discussed in detail in Ref. [2]. The schematic of a cross-sectioned test sample with the numbering of solder interconnects is shown in Fig. 1b. For in situ testing,

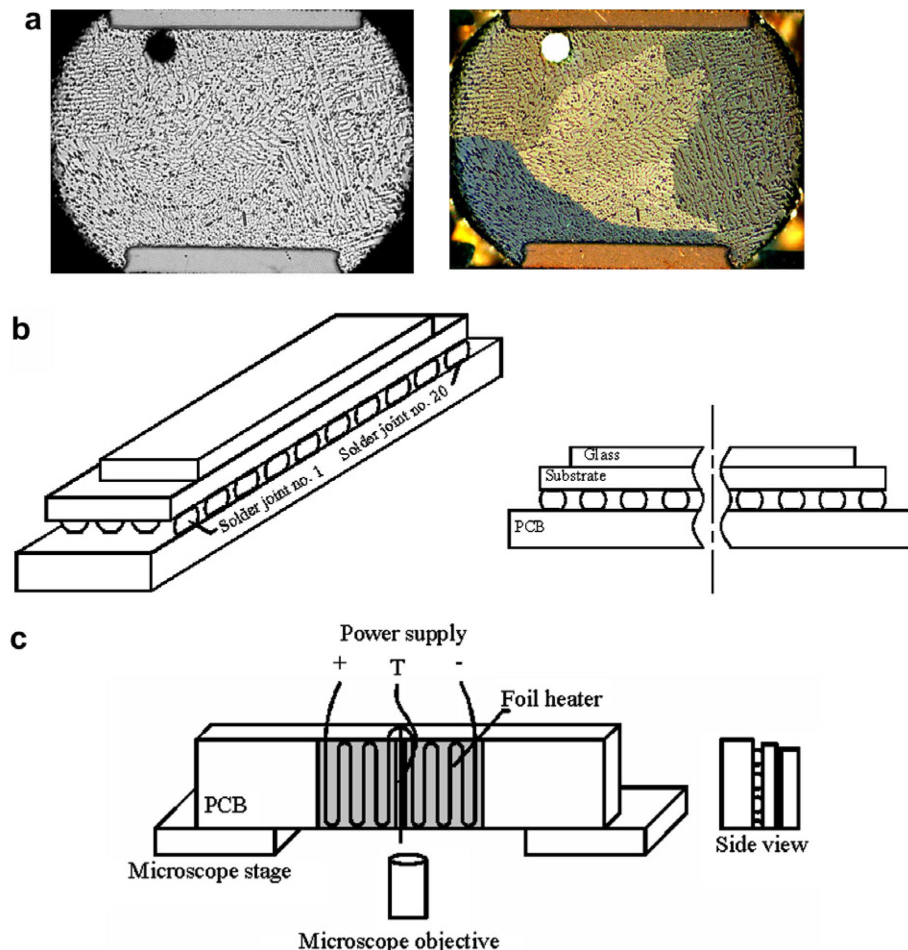

Fig. 1. Schematic of the test sample and experimental set-up. (a) BF and XP images of the cross-section of a solder interconnect. (b) A schematic of the test sample. (c) Set-up showing heating of the PCB side of the test sample on the microscope stage.

Minco™ foil heaters were mounted on the PCB side of the cross-sectioned assembly to maximize the thermal expansion mismatch between the PCB and the package. It is noted that the resultant thermal expansion is a product of an effective CTE and the temperature change in the region. In this case, the package, which is composed of an organic substrate and glass (the PBGA package) or a ceramic substrate (the CBGA package) above the solder interconnects, has a lower effective CTE compared with that of PCB while the temperature change in the package during thermal cycling is lower than that in the PCB.

2.2. Procedure

The assembly with foil heaters was placed on the optical microscope before the heaters were turned on. BF digital images of the interconnects were captured at room temperature in various magnifications as the reference images for DIC. Also, the images were taken under an XP to discern different grains [2]. The foil heaters were powered with a DC current from a power supply. The current was varied until the thermocouple attached on the PCB side of the assembly showed a steady-state temperature readout of 100 °C (at 0.3 A). After a dwell time of 10 min at 100 °C, the final sets of images were captured at the same magnifications. The two BF (converted to grayscale) images taken at room temperature and at 100 °C were used for DIC to quantify deformations and strains on the solder interconnect due to the thermal loading. The measured deformations and strains were then correlated with the grain distribution (or formation) as obtained from the XP images.

3. Results and analysis

The deformation and strain distribution at different locations of cross-sectioned interconnects have been examined. The images under the XP revealed that the majority of solder interconnects are multiple grained while a few appear to be single grained. Solder interconnects #1 and #3 (Fig. 2a and b) of the PBGA package appeared to be single and multiple grained, respectively, on the cross-sectioned plane.

When the foil heaters were powered, thermomechanical stresses were imposed upon the solder interconnects. These stresses are the result of the thermal expansion mismatch of the package and the PCB, the thermomechanical properties of intermetallics and the anisotropy in thermomechanical

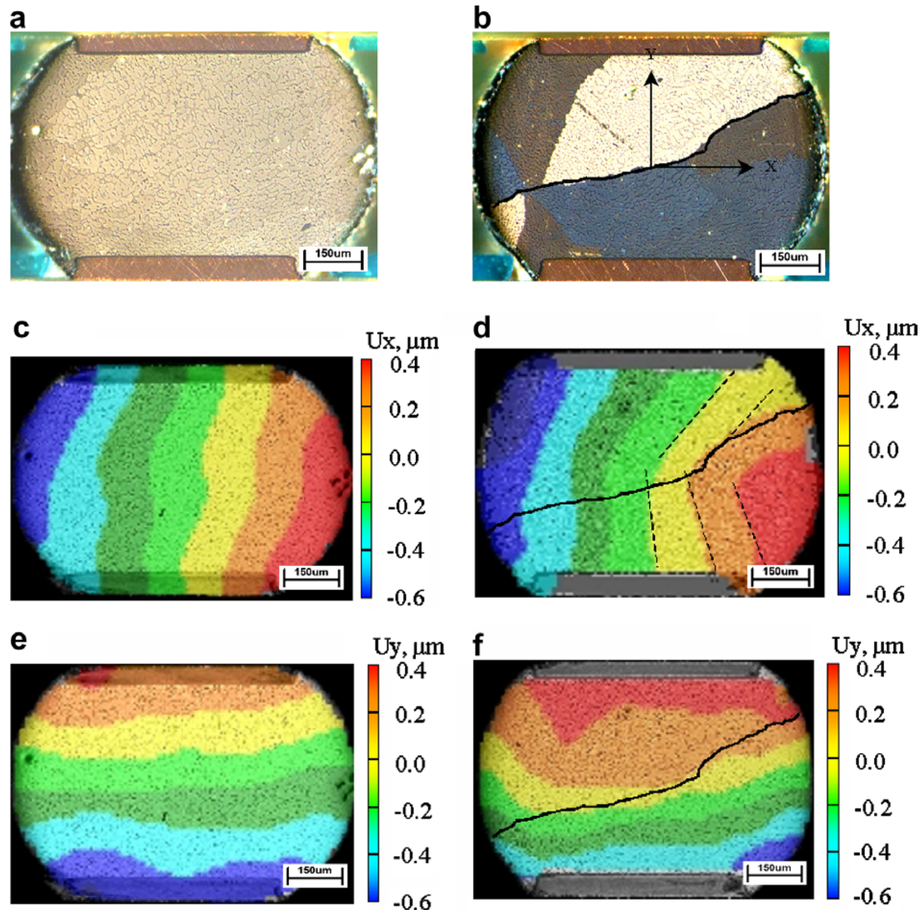

Fig. 2. (a, b) XP image; (c, d) *X*-displacement; and (e, f) *Y*-displacement contour plots as obtained from DIC for PBGA interconnect #1 (single grain, left) and interconnect #3 (multi-grain, right) in situ. The PCB side of the sample was heated from room temperature to 100 °C.

properties of different grains. Although there was a temperature gradient between the package and the PCB, it is reasonable to assume a uniform temperature within a solder interconnect considering the high thermal conductivity of the solder material.

Unlike solder interconnect #1, most of the other solder joints show a formation of multiple grains in the cross-section. Fig. 2b shows a 100× magnified XP image of the multi-grained solder interconnect #3, where the different grain orientations are shown by different colors. It should be noted that the same color indicates the same grain orientations. The pattern of grain distribution in Fig. 2b shows a good example of cyclic twinning around the [0 1 0] axis. This phenomenon was reported previously by Lehman et al. [7]. These solder interconnects comprise multiple grains, but with highly correlated orientations. Each twin segment (grain) is rotated 60° with respect to its neighbor. All the twin segments share a common [0 1 0] twin rotation axis. For a homogeneous and free-standing sphere heated to a uniform temperature, there will be no mechanical stresses built up. However, for a multi-grained sphere like the one in Fig. 2b (also known as Kara's beach ball), a temperature loading by itself generates mechanical stresses along the grain boundaries due to the anisotropy of differently orientated grains.

The deformation of solder interconnects under a thermal loading was quantified by DIC. Fig. 2c and e shows the uniform X (horizontal) and Y (vertical) displacement contours on the single-grained interconnect #1 when the PCB side of the package was heated to 100 °C. At the steady-state, the solder temperature was about 65 °C, which resulted in a temperature difference (ΔT) of 40 °C. The X- and Y-directional displacement contours shown in Fig. 2 are a result of free thermal expansion associated with this ΔT and the mechanical restraints on the joints. When the material is homogeneous, it is natural to expect uniform distribution of deformation under a certain global loading. The measured deformation contours of the single-grained interconnect #1 are quite uniform, as expected. There are some variations near the solder–pad interface area and these can be attributed to the mechanical restraints on the interconnect. The X-displacement mismatch between the top and the bottom of the solder interconnect, as evident from the inclination of the displacement contours, is about 0.2 μm. This inclination is attributed to the shear because of the CTE mismatch between the package region and the PCB.

Fig. 2d and f shows the deformation contours in the X- and Y-directions for the multi-grained solder interconnect #3. A black line is sketched in Fig. 2b to highlight the location of some grain boundaries. The slope of the X-displacement contour is not uniform, unlike in the case of the single-grained interconnect (Fig. 2c). It is different in the grain above the black line than in the grain below the line. This indicates that some grains undergo more shear deformation and/or thermal expansion along a certain direction than the others and this difference is governed by the relative orientation of the c-axes of the grains, and hence the thermomechanical anisotropy of the solder material.

Fig. 3 shows contour plots of von Mises strain distribution on the interconnects. In the case of the single-grain interconnect, which is homogeneous, the von Mises strain distribution shows a uniform value of about 0.4%. Slight variations along some random locations could be due to the effect of intermetallic precipitates, the presence of small low-angle grain boundaries and the inherent noise associated with the measurement technique, along the edges of the measurement surface. In the case of the multi-grained solder interconnect, DIC shows a distinct variation of von Mises strain along the grains above and below the dark line. The grain above the line shows an average strain value of 0.2% while the one below the line shows a value of about 0.45%. This mismatch in strain between the neighboring grains has to be accommodated by their grain boundary via grain boundary sliding or plastic work accumulation after several such cycles. This result supports the hypothesis that a failure crack propagates along the grain boundary after several thermomechanical cycles.

This non-uniformity in deformation is primarily attributed to the anisotropic nature of tin at the grain level. The linear CTE of tin along the [1 0 0] and [0 1 0] directions (a- and b-axes) is 15.4 ppm °C^{-1}, while it is 30.5 ppm °C^{-1} along the [0 0 1] direction (c-axis) [2–4]. Also, the Young's modulus of tin along the [1 0 0] and [0 1 0] directions is 23 GPa and that along the [0 0 1] direction is 70 GPa [3,4]. This anisotropy provides deformation variation in a

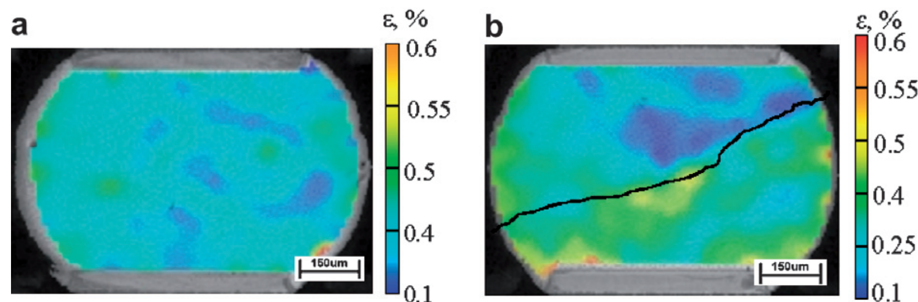

Fig. 3. von Mises strain contour plot as obtained from DIC for PBGA interconnect #1 (single grain), (a) and interconnect #3 (multi-grain), (b) in situ. The sample was heated from room temperature 25 °C to 100 °C.

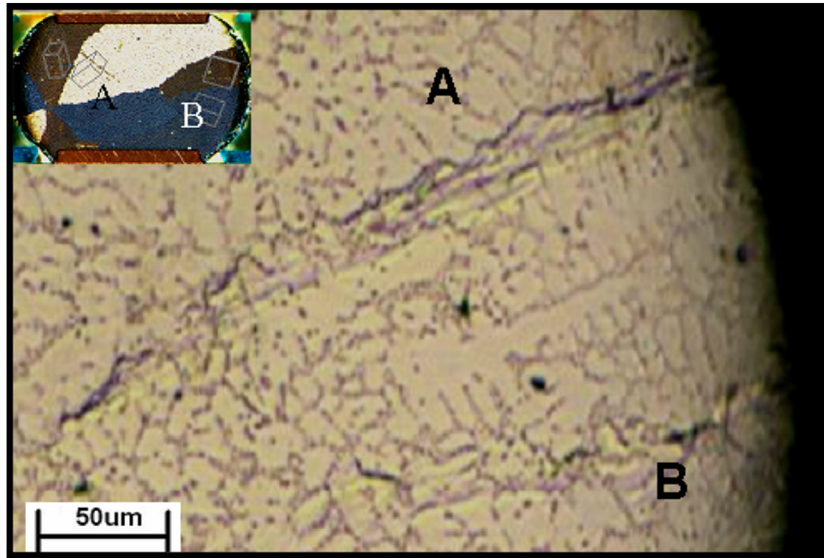

Fig. 4. Plastic deformation along the grain boundaries after 35 thermal cycles of 125 °C to −40 °C for multi-grain solder interconnect #3.

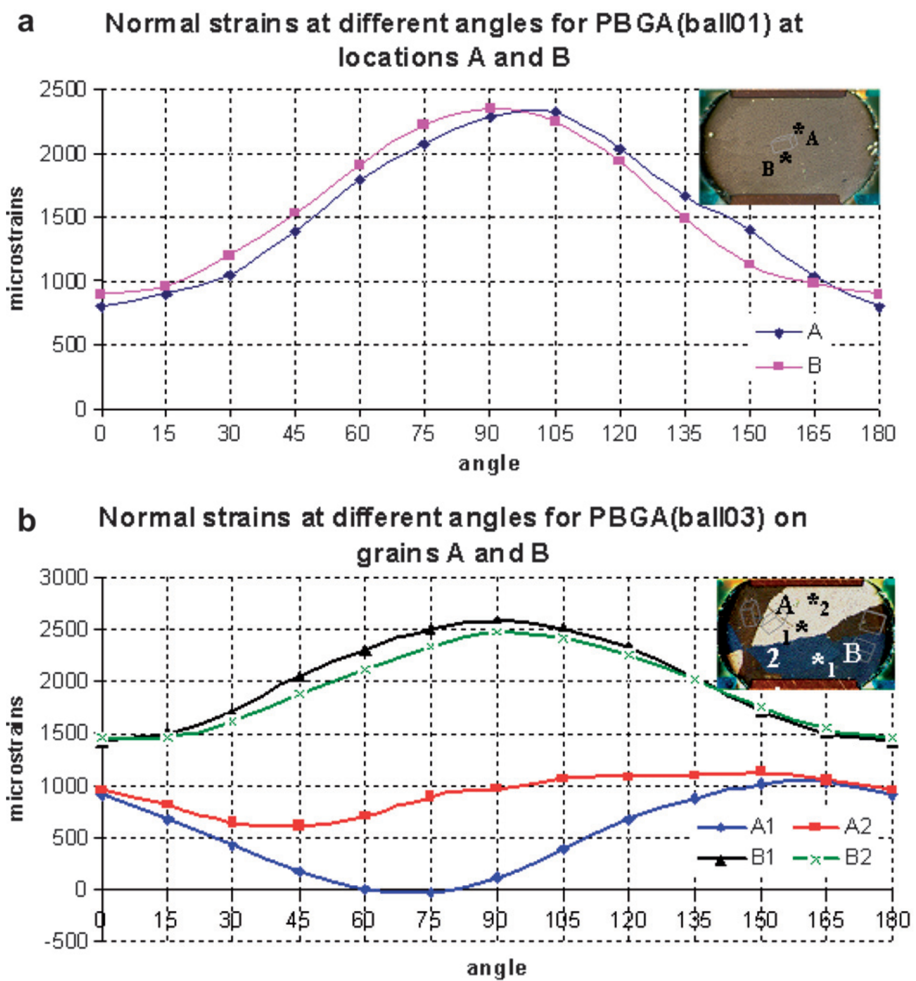

Fig. 5. Angular variation of normal strain in small elements at different locations when the package was heated from room temperature to 100 °C for: (a) single-grained PBGA interconnect #1, showing the same strain variation in different directions; and (b) multi-grained PBGA interconnect #3, showing the different strain variation in different grains.

given interconnect composed of a few grains of different orientations. It is not straightforward, however, to predict the deformation pattern in a given cross-section due to the unknown three-dimensional geometry of each grain. A combination of experimental and numerical approach is being exercised to predict the apparent deformations of a given solder interconnect under thermomechanical loading [14].

Fig. 4 shows a magnified image of the right hand side region of grains A and B. It reveals permanent plastic deformation (or strain accumulation) along the grain boundaries after the sample was subjected to 35 thermal cycles of −40 to 125 °C. The strain mismatch in adjacent grains, as evident in the von Mises strain contour of Fig. 4b, led to permanent plastic deformation along the boundaries of the grain (Fig. 4).

In Fig. 5a, the angular strains for two random locations, A and B, are plotted for comparison. Here, the angular strains are the extensional strains along the length of angled small line segment (ideally it should be a spot) with respect to the horizontal (X-axis). As shown in the plot, the angular strains are maximum at 2350 microstrains along

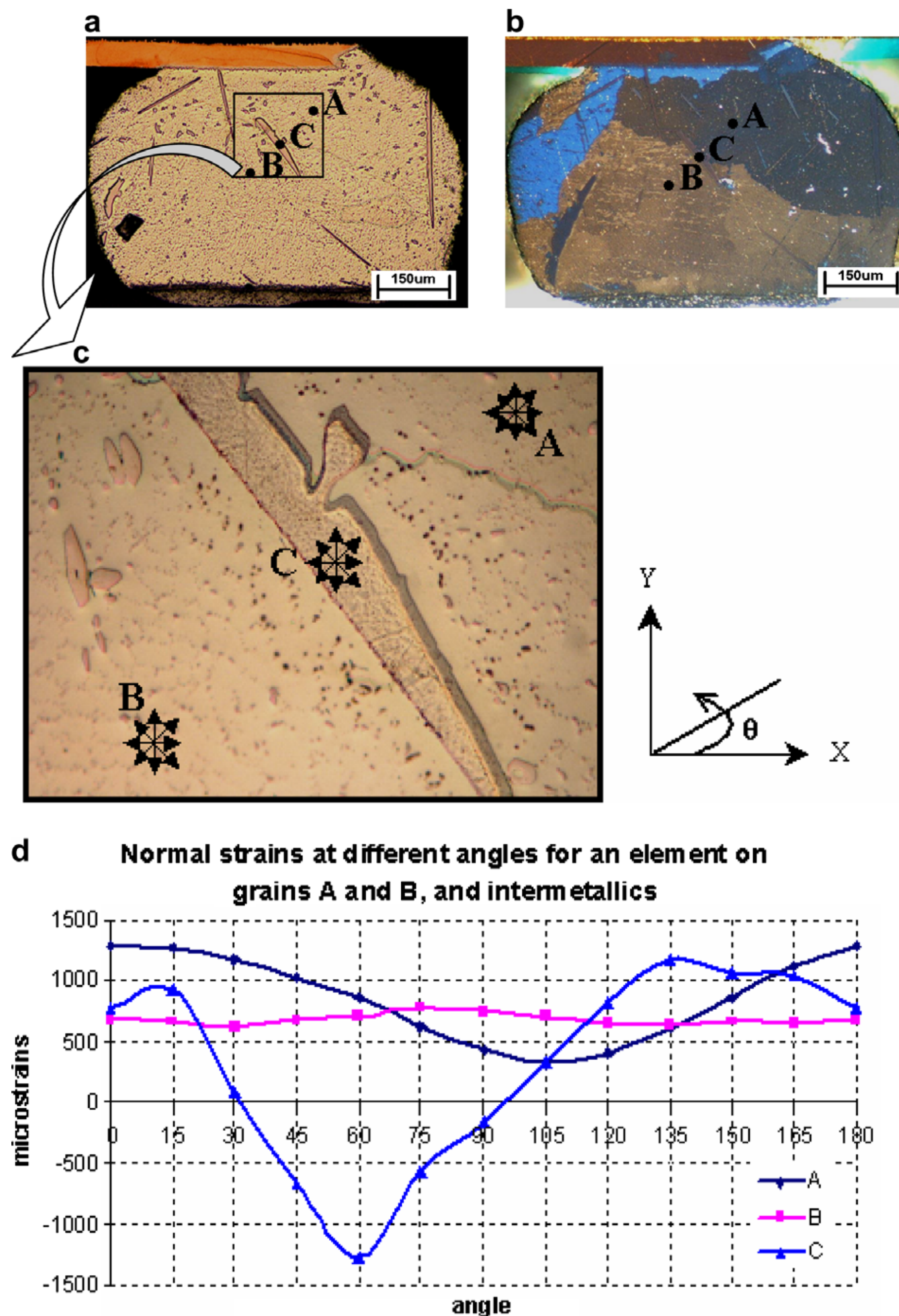

Fig. 6. CBGA interconnect #8. (a, b) Location of grains and Ag_3Sn plate; (c) BF image of Ag_3Sn plate at 1000× magnification; and (d) angular variation of strain at different locations when the sample was heated to 100 °C.

about 100° and minimum along 0° (parallel to the pads) for both locations A and B. The direction of maximum normal strain at location B is slightly offset from the one of location A and could be the influence of bending and shear loading in addition to the unknown three-dimensional effect of the grain(s). The directions of maximum or minimum normal strains are governed by the orientation of the *c*-axis in the cross-section, which determines the effective CTE and stiffness in that direction. The deformation of the interconnect is a result of mechanical strain by bending force and free thermal expansion of the solder material.

The same angular strain analyses were conducted for the multi-grained solder interconnect #3 (Fig. 5b). The direction of maximum normal strain in grain B is along 90°, while it is along 150° in the case of grain A. However, for two locations, 1 and 2, in the same grain the normal strain distribution is similar; this was also observed in the case of the single-grained interconnect (Fig. 5a). A slight variation in two points in grain A could be because of the pad effect or the grain shape in the third dimension. The direction of the maximum normal strain in the element is also governed by the effect of orientation of different neighboring grains in addition to other factors discussed earlier for the single-grained interconnect. The result shows that the strain distribution at different regions (A and B) is apparently different, while strains at the same region (1 and 2) have the same trend. It is evident that the difference in strain distribution in different grains is due to the anisotropic nature of the CTE and Young's modulus of each grain, even when the joint is subjected to a uniform thermomechanical loading. The strain mismatch at the two adjacent locations, A1 and B1, across the boundaries between the two grains, is considerably high, about 2000 microstrains. Hence, after a number of thermal cycles, this variation of strain distribution in adjoining grains can lead to plastic strain accumulation and, eventually, to crack initiation during thermal cycling along the grain boundary (Fig. 4).

3.1. Strains at and around the intermetallics

The inhomogeneous and anisotropic SAC solder interconnects are further complicated by the intermetallics. A further detailed study of strain distribution at and around the bigger intermetallics (Ag_3Sn plates) was conducted. As shown in Fig. 6, a region where two grains met and a bigger intermetallic plate existed was used for this analysis.

A larger primary intermetallic plate (Ag_3Sn) was imaged at room temperature and 100 °C with 1000× magnification and the two images were correlated to obtain deformation and strain distribution. Angular strain distribution is presented for differently orientated grains (at locations A and B) and an Ag_3Sn plate (at location C) in Fig. 6.

The strain field at the intermetallic (at location C) is very different from that in the neighboring grains (at locations A and B). It shows a fairly constant strain of 700 microstrains in all the angular directions for grain B, while grain A shows a minimum strain value of 300 microstrains at 105° and a maximum of 1300 microstrains at 0°. The difference in angular strains between the two neighboring grains could be big as shown in Fig. 5b. In this case, however, the proximity of the two points (A and B) and physical displacement continuity made the strain difference between the two locations look smaller in the plot.

An interesting strain distribution is observed at the larger primary intermetallic. The Ag_3Sn plate is inclined at about 125° from the horizontal axis and maximum and minimum angular strains are obtained at 60° (compressive) and 135° (tensile), respectively, with the amount of 1200 microstrains. The strain mismatches between the intermetallic and the neighboring grains (points A and B, Fig. 6c) are attributed to the size and location of the intermetallic plate and orientation of the neighboring grains. It was reported that the primary intermetallics could be the sites of crack initiation and propagation during thermal cycling, with the severity depending on the size of the intermetallics and their location with respect to the grain boundary and pad area [10]. Similar results in terms of strain and deformation mismatch along different grains and intermetallics were obtained when the same samples were subjected to multiple deep thermal cycles (−45 to 125 °C) [12].

4. Conclusion

A combination of optical microscopy and DIC was adopted to characterize the deformations and strains of board-level SnAgCu solder interconnects. The results were correlated with the distribution of different grains and their orientations.

Strain within a solder interconnect varied significantly in different grains and at and around the intermetallics under a thermomechanical loading. This anisotropic and nonhomogeneous distribution of deformation resulted in plastic deformation (or strain accumulation) along the grain boundaries and near the primary intermetallic precipitates during thermal cycling. This explains a mechanism of crack initiation and propagation along the grain boundaries and larger primary intermetallics after several thermal cycles. A further extension of this technique combined with three-dimensional numerical modeling considering the anisotropy would provide a better understanding of the failure mechanism and help to build more accurate reliability models of lead-free solders. This would ultimately contribute towards developing optimized process conditions to form different grain structures and intermetallic sizes, and improve the fatigue life of such joints.

References

[1] Subramanian KN, Lee JG. Effect of anisotropy of tin on thermomechanical behavior of solder joints. J Mater Sci: Mater Electron 2004;15:235–40.

[2] Park SB, Dhakal R, Lehman LP, Cotts EJ. Grain deformation and strain in board-level SnAgcu solder interconnects under deep thermal cycling. IEEE CPMT, in press.
[3] Park SB, Dhakal R, Lehman LP, Cotts EJ. Grain formation and intergrain stresses in a Sn–Ag–Cu solder ball. In: Proceedings of ASME InterPACK, San Francisco, CA, 2005.
[4] Matin MA, Cohen EWC, Vellinga WP, Geers MGD. Correlation between thermal fatigue and thermal anisotropy in a Pb-free solder alloy. Scripta Mater 2005;53:927–32.
[5] Rayne JA, Chandrasekhar BS. Elastic constants of β tin from 4.2 K to 300 K. Phys Rev 1990;115(63):1658–63.
[6] Henderson DW et al. The microstructure of Sn in near eutectic Sn–Ag–Cu alloy solder joints and its role in thermomechanical fatigue. J Mater Res 2004;19(6):1608–12.
[7] Lehman LP, Athavale SN, Fullem TZ, Giamis AC, Kinyanjui RK, Lowenstein M, et al. Growth of Sn and intermetallic compounds in Sn–Ag–Cu solder. J Electron Mater 2004;33(12):1429–39.
[8] Henderson DW, Gosselin T, Sarkhel A. Ag_3Sn plate formation in the solidification of near ternary eutectic Sn–Ag–Cu alloys. J Mater Res 2002;17(11):2775–8.
[9] Telang AU, Bieler TR, Lucas JP, Subramanian KN, Lehman LP, Xing Y, et al. Grain boundary character and grain growth in bulk tin and bulk lead-free solder alloys. J Electron Mater 2004;33(12):1412–23.
[10] Kim KS, Huh SH, Suganuma K. Effects of intermetallics compounds on properties of Sn–Ag–Cu lead free solder joints. J Alloys Compd 2002;1.
[11] Sutton MA, McNeill SR, Helm Jeffrey D, Chao Yuh J. Advances in two-dimensional and three-dimensional computer vision, photomechanics. Top Appl Phys 2000;77:323–72.
[12] Schmidt T, Tyson J, Galanulis K. Full-field dynamic displacement and strain measurement using advanced 3D image correlation photogrammetry. Exp Techniques 2003;Part I: vol. 27(3):47–50. 2003;Part II: vol. 27(4):p. 44–7.
[13] Shi X, Pang HLJ, Zhang XR, Liu QJ, Ying M. In situ micro-digital image speckle correlation technique for characterization of materials' properties and verification of numerical models. IEEE Trans Compon Pack Technol 2004;27:659.
[14] Park SB, Dhakal R, Gao J. Finite Elements analysis of three-dimensionally formed multiple grained SAC interconnects. J Exp Mech, in preparation.